Theoret. Comput. Fluid Dynamics (2004) 18: 183–196
Digital Object Identifier (DOI) 10.1007/s00162-004-0124-6

Theoretical and Computational Fluid Dynamics

Original article

Superfluid Couette flow in an enclosed annulus

Karen L. Henderson[1], Carlo F. Barenghi[2]

[1] School of Mathematical Sciences, University of the West of England, Bristol, BS16 1QY, UK
[2] School of Mathematics, University of Newcastle, Newcastle Upon Tyne, NE1 7RU, UK

Received September 5, 2003 / Accepted May 25, 2004
Published online September 1, 2004 – © Springer-Verlag 2004
Communicated by H.J.S. Fernando

Abstract. The Couette configuration of a fluid contained between two rotating concentric cylinders has proved useful to test and validate the HVBK equations which govern the motion of superfluid helium II. We critically review the current understanding of the superfluid Couette problem and compare theory and experiment, distinguishing between the results obtained with infinitely long cylinders and those obtained at small aspect ratio. After discussing some issues which are still unsolved, we point to what should be fruitful directions of further investigation which can be pursued in the Couette configuration.

Key words: Couette–Taylor problem, end effects, superfluid helium, HVBK equations

1 Introduction

Helium is a gas at ordinary room temperatures. To transform helium into a liquid it is necessary to cool it to about 4 Kelvin. If the temperature T is reduced further, at the critical value $T_\lambda = 2.1768$K (at saturated vapour pressure), a phase transition takes place, quantum effects become important and liquid helium acquires the remarkable property of superfluidity. Hereafter we shall only be concerned with this low temperature liquid phase (called helium II), which exists in the range $0 < T < T_\lambda$ and neglect the higher temperature liquid phase, which occurs for $T > T_\lambda$ (called helium I). See [1–4] for further details on the physical properties of helium II.

The physics of helium II (Bose–Einstein condensation) is interesting in its own right. Equally interesting are the engineering applications of helium II as a cryogenics coolant, due to the fact that there is no other substance available in liquid form near absolute zero. However the subject of this paper is not the fundamental physics nor the engineering applications, but rather the fluid dynamics aspect. Our aim is to critically review, put on firm ground and test what are thought to be the governing equations of superfluid hydrodynamics. Additional motivation for our work arises from recent and current experiments which have highlighted similarities and differences between superfluid turbulence and ordinary Navier–Stokes turbulence [5–9]. Although this paper is concerned only with laminar vortex flows, it is clear that a proper understanding of flows at low velocity underpins our understanding of turbulent flows.

The motion of helium II is usually modelled using Landau's two-fluid theory [10], in which the fluid is considered to be made up of two completely mixed components: the normal fluid and the superfluid. The

Correspondence to: K.L. Henderson (e-mail: karen.henderson@uwe.ac.uk)

former is related to thermally excited states (phonons and rotons) and is similar to a classical Navier–Stokes viscous fluid, whereas the latter is related to the quantum ground state and is similar to a classical Euler inviscid fluid. The superfluid velocity field is irrotational because it is proportional to the gradient of the quantum mechanical wave function. The total density of helium II is given by $\rho = \rho^n + \rho^s$ and is approximately constant, but the normal and superfluid densities ρ^n and ρ^s are strongly temperature dependent. At $T = 0$ the normal fluid component is absent and helium II is entirely superfluid ($\rho^n = 0$), whilst at $T = T_\lambda$ the superfluid component vanishes ($\rho^s = 0$) and helium II becomes helium I, which is an ordinary Navier–Stokes fluid.

If helium II is put in a simple cylindrical container and rotated with angular velocity Ω greater than some small critical value then Landau's original theory requires a subtle modification [3, 11]. The normal fluid behaves like any ordinary classical fluid and is put into solid-body rotation by the no-slip boundary conditions at the walls of the vessel. Hence it acquires vorticity 2Ω in the direction of the rotation axis. The superfluid cannot rotate like the normal fluid, instead it minimises its free energy by creating a lattice of vortex lines which are aligned along the axis of rotation. Since the axis of each filament is hollow within a region of radius $a_0 \approx 10^{-8}$cm, the superfluid becomes multiply connected and thus can acquire a net circulation whilst remaining irrotational. The key property of the vortex lines is that the circulation of the superfluid velocity field $\boldsymbol{v}^s$ along a closed path C around the axis of each line is a fixed quantity Γ (the quantum of circulation):

$$\oint_C \boldsymbol{v}^s \cdot \boldsymbol{dl} = \Gamma \tag{1}$$

where $\Gamma = 9.97 \times 10^{-4}\text{cm}^2/\text{sec}$ is the ratio of Planck's constant and the mass of one helium atom. The number of superfluid vortex lines per unit area is $N = 2\Omega/\Gamma$, thus approximating by discrete amounts (N times Γ) the vorticity 2Ω of the solid-body rotating normal fluid. In summary, the hydrodynamics problem which we consider involves the study of three classic fluid dynamic entities: a perfectly inviscid Euler fluid, a classical Navier–Stokes fluid and vortex lines. As far as we are concerned, the only visible effect of quantum mechanics is to guarantee that all the vortex lines have the same circulation Γ and the same vortex core radius a_0.

Because of the smallness of the quantum of circulation, even relatively weak rotational motions and eddies produce a large density L of vortex lines (defined as the length of line per unit volume, or equivalently as the number of vortices crossing the unit area). This means that, at least for laminar flows, the average separation between vortices $L^{-1/2}$ is usually smaller than any scale of interest in the flow. It is therefore useful to develop a set of macroscopic hydrodynamical equations for helium II which average over the presence of many individual vortex lines. This set of equations, referred to as the Hall–Vinen–Bekharevich–Khalatnikov (HVBK) model, was derived by a number of people over the years. Essentially, the HVBK model describes a continuum in which a fluid particle is a small but *macroscopic* region which is threaded by a high density of vortex lines, all pointing almost in the same direction [12–15]. This is an approximation, of course, because *microscopically*, that is to say on scales smaller than the scale described by the HVBK theory, each vortex line is a tiny hollow around which the superfluid velocity field is irrotational. The HVBK equations thus represent a coarse-graining of the original theory of Landau. Together with the vortex lines, the HVBK model introduces two new physical effects which are absent in Landau's original theory. The first is that the superfluid vortex lines scatter the thermal excitations, thus introducing a coupling force between normal fluid and superfluid components called the mutual friction force [16]; this effect is important in problems of heat flow because it leads to extra dissipation. The second effect is that the vortex lines have energy per unit length, that is tension. Because of the tension, the vortex lines which thread a fluid particle can oscillate (vortex waves), thus giving the superfluid an intrinsic springiness.

The aim of this paper is to give a critical overview of recent research involving the use of the HVBK model to investigate the flow of helium II in a Couette apparatus, that is the flow between two concentric rotating cylinders. Our aim is to put on firm ground and test the HVBK equations, which represent the best available model of superfluid hydrodynamics. We choose the Taylor–Couette flow because it has been used as a benchmark for fluid mechanics since Taylor's [17] pioneering work to investigate the transition from Couette flow to Taylor vortices, which together with previous work [18], established the use of the Navier–Stokes equations and the no-slip boundary conditions. Taylor–Couette flow is simple but not trivial, thus, unlike solid-body rotation (in which context the HVBK equations were first derived), all physical ingredi-

ents such as mutual friction and tension play a role in determining whether an instability occurs or not. This allows for a better understanding of the HVBK model. Furthermore, experimental data is available to test the theory. It must be stressed that progress in the helium II Couette problem has been slower than for classical fluids, due in part to problems of flow visualisation at such low temperatures, so we have much less information available than in the vast classical Taylor–Couette literature.

Experiments on helium II between concentric cylinders were first performed by Kapitza [19] in 1941; a review of all experiments involving helium II in Couette apparatus was written by Donnelly and LaMar [20]. In this article we shall expand on two types of experiments performed, which have been used for comparison against theoretical predictions. Early Taylor–Couette experiments were concerned with determining the viscosity of helium II by measuring the torque exerted by the flow on the stationary cylinder. A break in the linear dependence of the torque with the angular velocity of the rotating cylinder is taken to denote a transition from one flow pattern to another. The other experimental technique, that of measuring the extra attenuation of a second sound wave, can be used to probe the superfluid vorticity. Second sound waves occur when there is a periodic counterflow between the normal fluid and superfluid, which corresponds to a temperature and entropy wave at approximately constant density and pressure. Angular velocity is plotted against the attenuation factor and breaks in the curve are interpreted as transitions in the flow. By measuring the extra attenuation of second sound waves in the axial, azimuthal and radial directions it is theoretically possible to get an idea of the number and direction of the quantised vortex lines. In practice the information obtained in the experiments is less complete than this.

The plan of the paper is as follows. The HVBK model is presented in Sect. 2. Linear stability calculations and nonlinear solutions in the limit of infinitely long cylinders are presented in Sect. 3 and compared to experiments. The apparent discrepancy between theory and experiments at low temperatures is explained in terms of end effects, which motivate the calculations at finite (short) aspect ratios (in which vortex lines can be perpendicular to boundaries) presented in Sect. 4. These calculations reveal various anomalous flow patterns, but the last part of Sect. 4 shows that if the aspect ratio is large enough the results of the infinitely long cylinders theory are recovered. Finally, Sect. 5 summarises our understanding of the HVBK model, lists open questions which still need to be answered, and describes directions of further work.

2 Model

The isothermal, incompressible HVBK equations may be written as:

$$\frac{\partial \boldsymbol{v}^n}{\partial t} + (\boldsymbol{v^n} \cdot \nabla)\boldsymbol{v}^n = -\nabla p^n + \nu^n \nabla^2 \boldsymbol{v}^n + \frac{\rho^s}{\rho}\boldsymbol{F}, \tag{2}$$

$$\frac{\partial \boldsymbol{v}^s}{\partial t} + (\boldsymbol{v^s} \cdot \nabla)\boldsymbol{v}^s = -\nabla p^s + \boldsymbol{T} - \frac{\rho^n}{\rho}\boldsymbol{F}, \tag{3}$$

$$\nabla \cdot \boldsymbol{v}^n = 0, \quad \nabla \cdot \boldsymbol{v}^s = 0, \tag{4}$$

where $\boldsymbol{v}^n$ is the normal fluid velocity, p^n, p^s are effective pressures and ν^n is the kinematic viscosity of the normal fluid. What makes the HVBK equations different from Landau's two-fluid equations is the existence of the *macroscopic* vorticity field

$$\boldsymbol{\omega}^s = \nabla \times \boldsymbol{v}^s, \tag{5}$$

and the introduction of the mutual friction force $\boldsymbol{F}$ and the vortex tension force $\boldsymbol{T}$. Essentially, the superfluid vorticity $\boldsymbol{\omega}^s$ is a measure of how many vortex lines are contained in a given small region of fluid and point along a particular direction. We define $\widehat{\boldsymbol{\omega}}^s = \boldsymbol{\omega}^s/|\boldsymbol{\omega}^s|$ to be the unit vector in the direction of superfluid vorticity. The mutual friction force is

$$\boldsymbol{F} = \tfrac{1}{2}B\widehat{\boldsymbol{\omega}}^s \times (\boldsymbol{\omega}^s \times (\boldsymbol{v}^n - \boldsymbol{v}^s - \nu^s \nabla \times \widehat{\boldsymbol{\omega}}^s)) + \tfrac{1}{2}B'\boldsymbol{\omega}^s \times (\boldsymbol{v}^n - \boldsymbol{v}^s - \nu^s \nabla \times \widehat{\boldsymbol{\omega}}^s) \tag{6}$$

where B, B' are known temperature-dependent mutual friction parameters [4]. This force describes the interaction between the normal fluid and vortex lines. The vortex tension force may be written as

$$\boldsymbol{T} = -\nu^s \boldsymbol{\omega^s} \times (\nabla \times \widehat{\boldsymbol{\omega}}^s) \tag{7}$$

and reflects the energy in the vortex lines. The vortex tension parameter $\nu^s = (\Gamma/4\pi)\log(b_0/a_0)$ has the same dimension as kinematic viscosity, but physically it is very different; it represents the ability of a vortex line to oscillate due to vortex waves which can be excited on the vortex lines themselves. Finally the quantity $b_0 = (|\boldsymbol{\omega}^s|/\Gamma)^{-1/2}$ measures the typical inter-vortex spacing.

The HVBK equations have two interesting limits. If $T \to T_\lambda$, then $\rho^s/\rho \to 0$, $\rho^n/\rho \to 1$, helium II becomes entirely 'normal' and the normal fluid Eq. (2) reduces to the classical viscous Navier–Stokes equation. Vice versa, if $T \to 0$, then $\rho^n/\rho \to 0$, $\rho^s/\rho \to 1$ and helium II becomes entirely 'super'; in this limit, if we also set Planck's constant equal to zero, then Γ and ν^s vanish and the superfluid Eq. (3) reduces to the classical Euler equation.

We consider a sample of helium II held at temperature T and confined radially between two concentric cylinders of inner and outer radius R_1 and R_2, and axially between two fixed plates which are separated by a distance H. The top and bottom plates and the outer cylinder are held stationary and the inner cylinder rotates at constant angular velocity Ω_1. Results will be presented for the radius ratio, $\eta = R_1/R_2 = 0.976$ as in the experimental apparatus of Swanson and Donnelly [21]. The key parameters of the system are the Reynolds number of the inner cylinder, $\mathrm{Re} = \Omega_1 R_1 (R_2 - R_1)/\nu^n$, the aspect ratio, $h = H/(R_2 - R_1)$ and the temperature, T. Hereafter we shall use cylindrical coordinates (r, ϕ, z).

3 Results at infinite aspect ratio

3.1 Linear theory

In the case of flow between infinite cylinders ($h \to \infty$), Couette flow, given by

$$\boldsymbol{v}_c = (Ar + C/r)\,\widehat{\mathbf{e}}_\phi \tag{8}$$

(where $\widehat{\mathbf{e}}_\phi$ is the unit vector in the azimuthal direction) is an exact solution of the HVBK equations for both the normal fluid and superfluid (provided that Ω_1 is greater than a small critical value at which vortex lines first appear). The values of A and C are determined by the no-slip boundary conditions imposed on the normal fluid at the cylinder walls, which are:

$$v_r^n = 0 \quad \text{at} \quad r = R_1 \text{ and } R_2 \tag{9}$$

$$v_\phi^n = \Omega_1 r \quad \text{at} \quad r = R_1 \tag{10}$$

$$v_\phi^n = 0 \quad \text{at} \quad r = R_2 \tag{11}$$

$$v_z^n = 0 \quad \text{at} \quad r = R_1 \text{ and } R_2. \tag{12}$$

The superfluid, being inviscid, is not required to satisfy such boundary conditions; the only restriction is that there is no penetration through the boundary:

$$v_r^s = 0 \quad \text{at} \quad r = R_1 \text{ and } R_2. \tag{13}$$

From Eq. (8) it can be seen that in the Couette state the superfluid vorticity is purely axial and has a magnitude of $2|A|$.

The first pioneering attempt to calculate the stability of helium II flowing between rotating concentric cylinders was made by Chandrasekhar and Donnelly [22], who did not make contact with the experiments because they failed to properly take into account the vortex tension force. Barenghi and Jones [23] and Barenghi [24] considered the linear stability of Couette flow with respect to infinitesimal perturbations of the form $\exp(\mathrm{i}m\phi + \mathrm{i}kz + \sigma t)$ where σ is the complex growth rate, m the azimuthal wavenumber and k the dimensionless axial wavenumber (expressed in units of $1/\delta$ where $\delta = R_2 - R_1$ is the gap width). Barenghi and Jones [23] found that if the inner cylinder rotates sufficiently fast, at a certain critical value $\mathrm{Re} = \mathrm{Re}_{\mathrm{crit}}$ the growth rate, Real (σ) of the axisymmetric $(m = 0)$ perturbation becomes positive, hence Couette flow becomes unstable. This transition corresponds to the onset of Taylor vortices for a classical fluid. In Fig. 1 we plot curves showing the stability boundaries of the axisymmetric mode against axial wavenumber k for (a) helium I (dotted), (b–d) helium II at temperatures $T = 2.16$ K, 2.1 K, 2.05 K, respectively (solid lines).

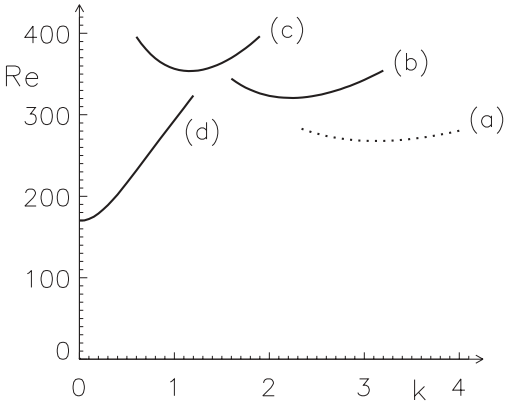

Fig. 1. Stability boundaries of **(a)** helium I (dotted), helium II (solid) at temperatures **(b)** $T = 2.16$ k, **(c)** $T = 2.1$ K, **(d)** $T = 2.05$ K

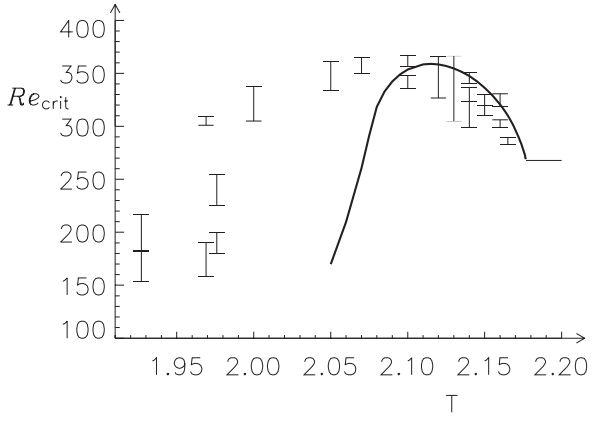

Fig. 2. Critical Reynolds number, $\mathrm{Re}_{\mathrm{crit}}$ as a function of temperature T (measured in Kelvin). Error bars: data of Swanson and Donnelly [21]; solid line: prediction from linear stability analysis [24]

The regions which are below and above each stability curve represent stable and unstable Couette flow respectively. Since helium I is a classical Navier–Stokes fluid, the dotted stability curve (a) represents the well-know transition from Couette flow to Taylor vortices (at this value of radius ratio). The critical Reynolds number $\mathrm{Re}_{\mathrm{crit}}$ and critical wavenumber k_{crit} are given by the minimum of each curve. For the sake of clarity only the bottom part of each stability curve has been plotted. From Fig. 1 we can see that helium II is more stable than helium I at temperatures close to T_λ and that the critical axial wavenumber decreases as the temperature is reduced.

The results of Barenghi and Jones [23] prompted further experiments [21] and good agreement between the predicted and measured values of $\mathrm{Re}_{\mathrm{crit}}$ was found [24], particularly for temperatures close to T_λ (see Fig. 2). Unfortunately, as is visible in Fig. 2, at lower temperatures ($T < 2.1$ K), although there is qualitative agreement between theory and experiment, the measured critical Reynolds numbers are larger than those predicted by the linear stability analysis. Barenghi and Jones argued that the discrepancy arises from the temperature dependence of the critical axial wavenumber k_{crit}. In the classical Taylor–Couette problem $k_{\mathrm{crit}} \approx \pi$, hence each individual Taylor vortex cell is approximately square (the extension in the axial direction is equal to the gap's size). In the case of helium II, Barenghi and Jones [23] found that $k_{\mathrm{crit}} \to \pi$ as $T \to T_\lambda$, as expected in the limit of a pure normal fluid. However, as the temperature is reduced, they found that k_{crit} decreases and tends to zero (see Fig. 3). This result suggests that the discrepancy between theory and experiments for $T < 2.1$ K is due to end effects; at low enough temperatures there are not enough Taylor vortex cells in the typical experimental apparatus, thus the infinite cylinder assumption breaks down. It is important to remark that this feature does not arise in the classical Taylor–Couette problem. It is important to note

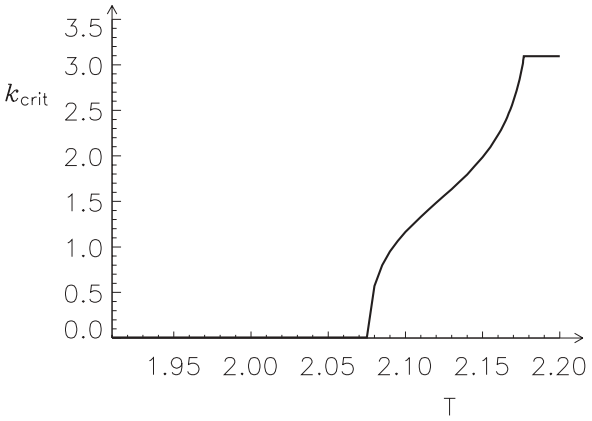

Fig. 3. Critical axial wavenumber, k_{crit} as a function of temperature T (measured in Kelvin)

that, due to the lack of direct flow visualisation of the helium II Couette problem, the elongation of the Taylor vortex cells is not immediately visible to the experimentalist.

3.2 Nonlinear solutions

The success of the linear stability analysis at temperatures close to T_λ validated the HVBK equations, at least in the linear regime, and opened the door to further study. Using the infinite cylinder assumption ($h \to \infty$), Henderson, Barenghi and Jones [25] numerically solved the HVBK equations for the first time and computed the nonlinear flow of helium II between infinite cylinders. The aim of the work was to obtain solutions for helium II corresponding to what would be Taylor vortices in a classical flow and to investigate what happens to the vortex lines. Only axisymmetric solutions were considered since linear theory predicts that, for rotation of the inner cylinder only, the axisymmetric mode onsets first. To solve the HVBK Eqs. (2–4), boundary conditions are required. The nonlinear problem is 6th order in both the normal fluid and superfluid; however, the linear problem is only 2nd order in the superfluid. Thus two further boundary conditions for the superfluid are needed in addition to the no penetration of the boundary (13) used successfully in the linear stability analysis. The extra boundary conditions employed are

$$\omega_\phi^s = 0 \quad \text{at} \quad r = R_1 \text{ and } R_2 \tag{14}$$

$$v_\phi^s = \Omega_1 r \quad \text{at} \quad r = R_1 \tag{15}$$

$$v_\phi^s = 0 \quad \text{at} \quad r = R_2. \tag{16}$$

Equations (14–16) force the superfluid vorticity to be purely axial at the cylinder walls. This is consistent with Couette flow, in which the vortex lines are purely axial throughout the flow and results in the mutual friction being small at the boundaries, which is an advantage numerically and helps the stability of the numerical scheme. The normal fluid satisfies the standard no slip boundary conditions (9–12) as for the linear model.

The HVBK equations were solved numerically using a pseudo-spectral method, based on expansions in Chebychev polynomials in the radial direction and trigonometric functions in the axial direction [26]. Results were obtained for angular velocities of up to 15% above the critical angular velocity at which linear theory predicts that Couette flow becomes unstable. Apart from the axial stretching of the Taylor cells, the normal fluid displays a velocity profile similar to that of a classical fluid, However, at lower temperatures, the superfluid velocity profile is markedly different to the classical case; instead of a meridional flow consisting of single pair of cells in each period, we find a more complex pattern of eddies and counter-eddies. Perhaps what is of most interest is the orientation of the vortex lines. The numerical results show that the superfluid vorticity is still predominantly axial and the deflection in the azimuthal direction is smaller than that in the radial direction. This is illustrated in Fig. 4a in which contour plots of the three components of superfluid vorticity at $T = 2.17$ K, Re $= 300$ are shown. The rotating inner cylinder is on the the left and the stationary outer cylinder is on the right. Results are plotted over a complete wavelength $\lambda = 2\pi/k$ where the axial

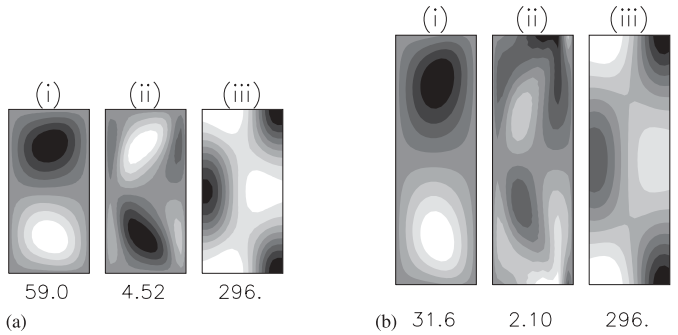

Fig. 4a,b. Components of superfluid vorticity: (i) ω_r^s, (ii) ω_ϕ^s, (iii) ω_z^s at $T = 2.17$ K, Re $= 300$ calculated using (**a**) the infinite cylinder code (plotted over a complete period: $0 < z/\delta < 2\pi/k$, where $k = 2.9$), (**b**) the finite aspect ratio code, taking $h = 6$ (plotted for $1.5 \leq z/\delta \leq 4.5$). The value printed underneath each plot corresponds to the average value of the absolute value of each field over the region plotted

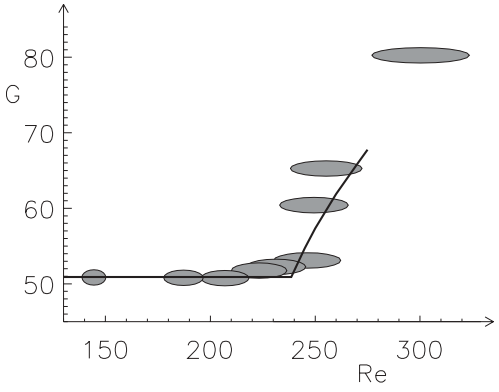

Fig. 5. Plot of dimensionless torque against Reynolds number for helium II at 2.1 K. Ellipses: experimental data of Donnelly [28]; solid line: numerical results

wavenumber is taken to be $k = k_{\text{crit}} = 2.9$ as predicted from linear theory. The value printed underneath each plot corresponds to the average value of the absolute value of each field over the region plotted. Light and dark regions correspond to positive and negative contour lines respectively.

The numerical results were compared with experiments in two different ways. Firstly by comparing the additional attenuation of a second sound wave due to the vortex lines and secondly by measuring the torque exerted on the outer cylinder. Henderson, Barenghi and Jones [25] compared the relative change in the azimuthal attenuation coefficient of second sound and found an order of magnitude correspondence between the experimental value of Swanson and Donnelly [21]. Henderson and Barenghi [27] compared torque measurements with those measured by Donnelly [28] at $T = 2.1$K. The results are presented in Fig. 5 in which the dimensionless torque G applied to the outer cylinder is plotted against Reynolds number. The solid line represents the results of the calculation and the ellipses represent the experimental data of Donnelly [28]. The observed break in the curve represents the onset of Taylor vortices and it can be seen that there is good agreement between the calculation and the experimental data in the nonlinear regime. This agreement further validated the HVBK model in the high temperature regime.

4 Results at finite aspect ratio

As discussed in Sect. 3.1, at low enough temperatures the cylinder ends need to be included in the model. This enables us to study how the vortex lines respond to a shear in the presence of boundaries which are both parallel and perpendicular to the natural axial direction of the vortex lines. Henderson and Barenghi [29] considered helium II contained in a unit aspect ratio ($h = 1$) Couette annulus and revealed unexpected flow patterns, some of which have similarities to anomalous modes known in the classical Taylor–Couette literature [30]. The axisymmetric form of the HVBK Eqs. (2–4) were solved using a finite difference approach

taking a regular grid in both the r and z direction. The boundary conditions on the curved cylinder walls were taken to be the same as for the infinite cylinder case (9–16). However extra boundary conditions are needed on the two end-caps, $z = 0$, H. For the normal fluid, standard no slip boundary conditions were imposed:

$$v_r^n = 0 \quad \text{at} \quad z = 0 \text{ and } H \tag{17}$$
$$v_\phi^n = 0 \quad \text{at} \quad z = 0 \text{ and } H \tag{18}$$
$$v_z^n = 0 \quad \text{at} \quad z = 0 \text{ and } H. \tag{19}$$

Whilst for the superfluid the following boundary conditions were used:

$$v_z^s = 0 \quad \text{at} \quad z = 0 \text{ and } H \tag{20}$$
$$\omega_r^s = 0 \quad \text{at} \quad z = 0 \text{ and } H \tag{21}$$
$$\omega_\phi^s = 0 \quad \text{at} \quad z = 0 \text{ and } H. \tag{22}$$

The first condition (20) ensures that there is no penetration of the superfluid through the boundary, whilst the last two conditions (21,22) correspond to perfect sliding of the vortex lines as discussed by Khalatnikov [2]. We shall present the results at finite aspect ratio in two parts. The low Reynolds number flow, which corresponds to the Couette state in the infinite cylinder case, is described in Sect. 4.1 and the transition to Taylor vortices is described in Sect. 4.2. Figures 6–9 show contour plots of various quantities for the complete cross-section of the annulus; $R_1 \le r \le R_2$, $0 \le z \le H$ with the inner/outer cylinder on the left/right respectively. The maximum value of each field is printed underneath the corresponding contour plot. Light and dark regions correspond to positive and negative contour lines, respectively.

4.1 Low Reynolds number flow

Henderson and Barenghi [29] considered the low Reynolds number flow of helium II in a unit aspect ratio Couette annulus and extended their work to consider moderate aspect ratios [34]. The main result is the anomalous motion of helium II when compared to the motion of a classical fluid. We shall highlight the key findings in this section.

The velocity profile obtained is a superposition of an azimuthal motion v_ϕ around the inner cylinder and a toroidal motion v_r and v_z in the vertical plane. The latter motion is in the form of a pair of cells similar to a Taylor vortex pair, but being caused by boundaries rather than a centrifugal instability, it is hereafter referred to as an Ekman cell pair. This toroidal motion may be visualised by introducing the stream function ψ such that

$$v_r^p = -\frac{1}{r}\frac{\partial \psi^p}{\partial z}, \qquad v_z^p = \frac{1}{r}\frac{\partial \psi^p}{\partial r} \tag{23}$$

where $p = n$, s represents the normal fluid, superfluid, respectively. The motion in the vertical (r, z) plane occurs along the streamlines, given by $\psi =$ constant.

In Fig. 6 we show contour plots of the stream function and azimuthal velocity of the normal fluid and superfluid for Re $= 100$, $h = 2$ at temperatures $T = 2.11$ K and $T = 2.17$ K, respectively. The first interesting result is that at low temperatures v_ϕ^s is almost z-independent (Fig. 6a(iv)). That is the superfluid moves around the cylinders in a column-like fashion, which is found to be due to the tension in the vortex lines [29]. This effect becomes less pronounced at higher temperatures when the superfluid component is smaller (Fig. 6b(iv)). In contrast v_ϕ^n is highly z-dependent as a result of the no-slip boundary conditions.

The second interesting result comes from looking at the Ekman cells in both the normal fluid and superfluid. In a classical fluid the primary flow is such that the two Ekman cells form with outflow at the centre and inflow at the ends of the cylinder. However it is possible to have anomalous modes in which the rotation is the opposite direction (the outflow is near the ends). The connection between the infinite and the finite Taylor–Couette problem and the existence of anomalous modes on a disconnected branch has been investigated [31–33]. These solutions occur at Reynolds numbers higher than the values which we have investigated. In the case of helium II the mutual friction is an extra physical ingredient, and it appears that it can switch which branch is the "primary" one. In principle one could pursue the search for a secondary branch. In

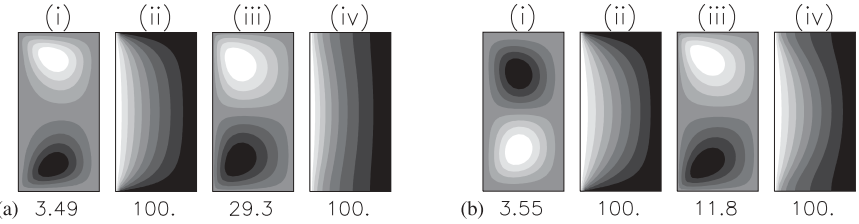

Fig. 6a,b. Contour plots of (i) ψ^n, (ii) v_ϕ^n, (iii) ψ^s, (iv) v_ϕ^s for Re $= 100$, $h = 2$ at (**a**) $T = 2.11$ K, (**b**) $T = 2.17$ K. The value printed underneath each plot corresponds to the maximum value of each field over the region plotted

the parameter region investigated, we find that the superfluid Ekman cells always rotate in a counter-classical way due to the mutual friction force, that is outflow occurs at the ends of the cylinder with inflow at the centre (Figs. 6iii(a,b)). It is also seen that the normal fluid Ekman cells rotate in a counter-classical way at lower temperatures (Fig. 6a(i)), but revert to a classical direction close to the transition temperature T_λ as one would expect (Fig. 6b(i)).

The effect of increasing the aspect ratio is illustrated in Fig. 7 where we plot contours of the stream function and azimuthal velocity of the normal fluid and superfluid at Re $= 100$, $h = 6$ at temperatures $T = 2.11$ K and $T = 2.17$ K respectively. At $T = 2.11$ K we see that the superfluid motion takes the form of a pair of counter-classically rotating Ekman cells (Fig. 7a(iii)). In contrast the normal fluid is in the form of four cells, with the outer cells rotating counter-classically (Fig. 7a(i)). The inner cells produce outflow at the centreline. At $T = 2.17$ K we see that the normal fluid motion takes the form of a pair of classically rotating Ekman cells (Fig. 7b(i)). In contrast the superfluid is in the form of four cells, with the outer cells rotating counter-classically as a result of the boundary conditions there (Fig. 7b(iii)). The inner cells rotate in such a way as to match the flow of the normal fluid at the centreline. At larger aspect ratios the column-like motion of the azimuthal component of superfluid velocity is still evident, though it is less pronounced (Fig. 7iv(a,b)).

4.2 Transition to Taylor vortices

Henderson and Barenghi [34] considered the transition from Ekman cells to Taylor vortices in an enclosed annulus. The transition point. $\mathrm{Re}^*_{\mathrm{crit}}$ was quantified by considering the break in the graph of the centreline average of v_r for both the normal fluid and superfluid. At $T = 2.17$K, $h = 6$ there is good agreement between the observed critical Reynolds number ($\mathrm{Re}^*_{\mathrm{crit}} \approx 275$) and that predicted by stability analysis in the infinitely long cylinders approximation ($\mathrm{Re}_{\mathrm{crit}} = 278.7$). The fully developed Taylor vortex flow is shown in Fig. 8 in which we plot contours of the stream function and azimuthal velocity of the normal fluid and superfluid at Re $= 300$. We can see that the normal fluid has split into six cells and that despite the superfluid having an additional weak pair of cells close to the ends of the cylinders in the (r, z) plane, the two fluids appear to match each other. The low Reynolds number flow (Re $= 100$) is plotted in Fig. 7b.

The previous calculation was repeated at the lower temperature of $T = 2.16$K for two different aspect ratios: $h = 4$ and $h = 6$. Contour plots of the stream function and azimuthal component of velocity of the normal fluid and superfluid are plotted for Re $= 310$ in Fig. 9. What is striking about these plots is that the normal fluid Taylor cells are elongated, developing two cells when $h = 4$ and four cells when $h = 6$. This is consistent with the linear stability analysis which predicts the critical axial wavenumber $k_{\mathrm{crit}} = 2.35$. The elongation of the Taylor cells was first predicted by Barenghi and Jones [23] and this is the first time that it has been observed numerically taking end effects into account. In contrast, the superfluid develops four and six cells at aspect ratios $h = 4$ and $h = 6$, respectively. Although the matching between the normal fluid and superfluid is not as pronounced as at higher temperatures, there is a similar structure to the velocity profiles of the two fluids away form the cylinder ends.

The transition to Taylor vortices is illustrated in Fig. 10 in which we plot the centreline average value of the radial component of the normal fluid against Reynolds number for (a) $h = 4$, (b) $h = 6$. Note that for the case of $h = 4$ the quantity $\langle v_r^n \rangle$ is positive because the normal fluid develops two classically rotating cells resulting in outflow at the centre. In contrast, when $h = 6$ the normal fluid develops four cells with the central two cells rotating in such a way as to produce inflow at the centre, thus $\langle v_r^n \rangle$ is negative. Linear stability analysis predicts $\mathrm{Re}_{\mathrm{crit}} = 310.7$, so the agreement is not as good as at higher temperatures due to

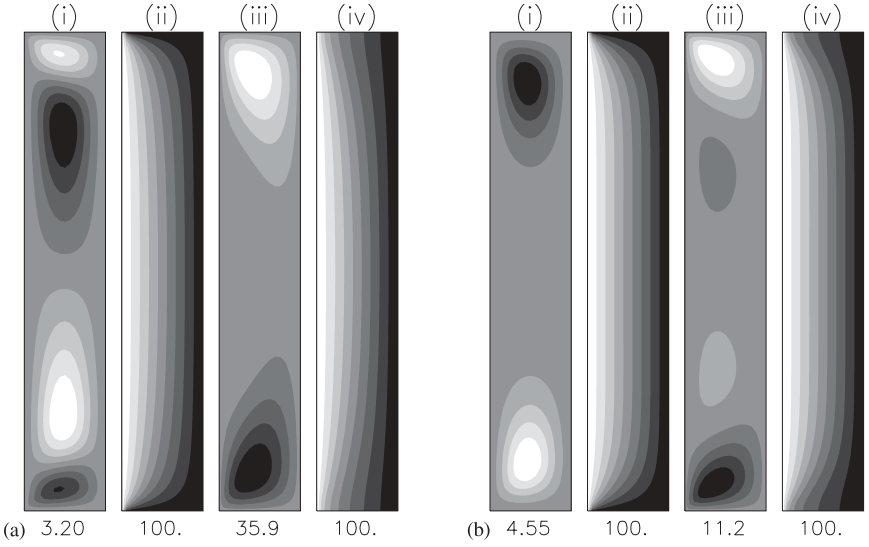

Fig. 7a,b. Contour plots of (i) ψ^n, (ii) v_ϕ^n, (iii) ψ^s, (iv) v_ϕ^s for Re $= 100$, $h = 6$ at (**a**) $T = 2.11$ K, (**b**) $T = 2.17$ K. The value printed underneath each plot corresponds to the maximum value of each field over the region plotted

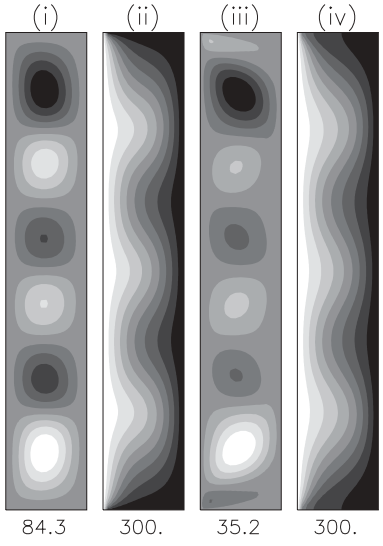

Fig. 8. Contour plots of (i) ψ^n, (ii) v_ϕ^n, (iii) ψ^s, (iv) v_ϕ^s at Re $= 300$, $h = 6$, $T = 2.17$ K. The value printed underneath each plot corresponds to the maximum value of each field over the region plotted

the elongation of the cells. It appears that at lower temperatures, larger aspect ratios need to be considered to make qualitative contact with the predictions of the linear stability analysis which assumes infinitely long cylinders.

We find that in general the superfluid vorticity is primarily axial and concentrated towards the ends of the cylinders close to the inner cylinder. This predicted result could be observed experimentally by measuring the extra attenuation of second sound waves due to the vortex lines at the centre and ends of the apparatus. As the Reynolds number is increased, there is a much larger deflection of the vortex lines in the radial direction. This is illustrated in Fig. 4b in which we plot the superfluid vorticity components of helium II at $T = 2.17$ K, $h = 6$ at the Reynolds numbers Re $= 300$ for the central region of the apparatus ($1.5 \leq z/\delta \leq 4.5$). This enables us to see what happens to the vortex lines in the centre of the apparatus away from the cylinder ends, where there is stronger shear which would make the contour lines in the middle of the apparatus less visible. The value printed underneath each plot corresponds to the average value of the absolute value of each field

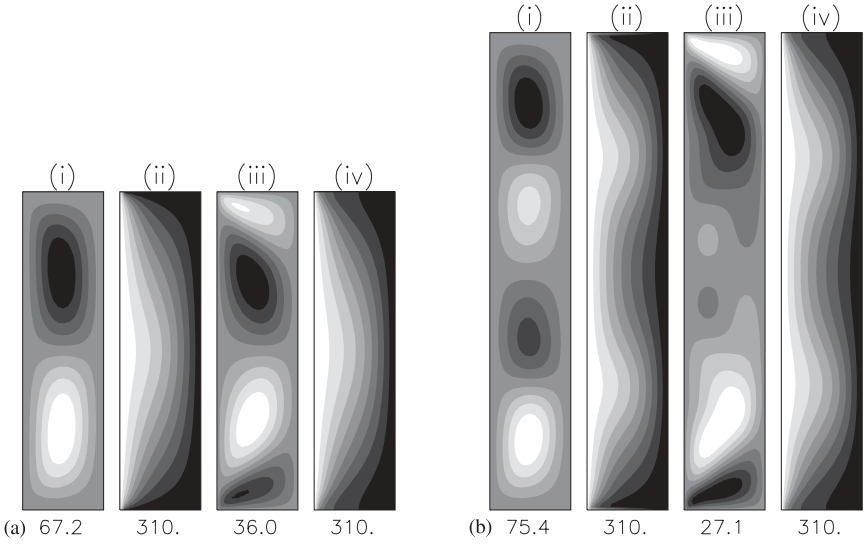

Fig. 9a,b. Contour plots of (i) ψ^n, (ii) v_ϕ^n, (iii) ψ^s, (iv) v_ϕ^s at $T = 2.16$ K, Re $= 310$ for (**a**) $h = 4$, (**b**) $h = 6$. The value printed underneath each plot corresponds to the maximum value of each field over the region plotted

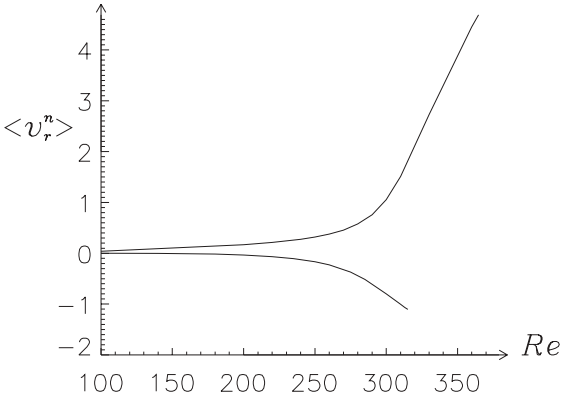

Fig. 10. Plot of the average values of v_r^n at the centreline $z = H/2$ against Reynolds number at $T = 2.16$ K and aspect ratio **(a)** $h = 4$, **(b)** $h = 6$

over the region plotted. Comparing the results with Fig. 4a, which was performed at the same temperature and Reynolds number but using the infinite cylinder code, we see that the vorticity pattern is similar to that found when considering the Taylor–Couette flow of helium II without end effects.

5 Discussion

The results which we have presented show that at relatively high temperatures there is fairly good quantitative agreement between the linearised HVBK theory and experiments, whereas at lower temperatures the agreement is qualitative only. Furthermore, at least at high temperatures, the HVBK model has been validated in the nonlinear regime too. These results are encouraging but there are still many important issues about the HVBK model which need to be addressed. The list below summarises points which need to be clarified and also possible avenues of further investigations:

Flow visualisation: On the experimental side, the major drawback remains the lack of direct flow visualisation in the difficult low temperature environment of helium II. In particular there is little information available about the motion of the normal fluid; the quantity which is generally measured and reported is the

superfluid vortex line density. Visualisation of the normal fluid pattern is necessary to test the effects predicted in sections 4.1 and 4.2, which depend on the relative balance of friction and tension forces. When studying the classical Taylor–Couette problem, introduction of flakes (Kalliroscope) or other small particles into the working fluid (usually oil or water), results in the Taylor vortices being clearly evident. Simple visualisation with ink revealed a long time ago that the critical (dimensionless) wavenumber is $k_{\rm crit} \approx \pi$ for which the Taylor vortex cells are approximately square. In contrast, the limited visualisation techniques available for helium II did not reveal that the Taylor cells become elongated at lower temperatures. The consequence of this effect (the value of $\mathrm{Re}_{\rm crit}$) became apparent only when predicted by the linear theory. Attempts have been made to visualise the flow pattern of helium II by adding small particles [35]. However this was only successful at high rotation rates (40 times the critical angular velocity at which linear stability analysis predicts Couette flow becomes unstable). Current work on this problem is based on Particle Image Velocimetry (PIV) [36–38] but the technique is still in the development stage and no results have yet appeared which can be used to test the HVBK theory. On the contrary, preliminary investigations suggest that more theoretical work is needed to interpret PIV data correctly; it is not clear whether the small particles trace the motion of the normal fluid or a combination of the motion of the normal fluid and superfluid.

Boundary conditions: A surprising feature which makes the HVBK equations different to the Navier–Stokes equations in the the Taylor–Couette problem is that the nonlinearities determine the order of the system of differential equations. The fully nonlinear HVBK equations are 12th order in the coupled normal fluid and superfluid system, but reduce to 8th order when linearised. In contrast, the classical Navier–Stokes equations are always 6th order, irrespective of the linearisation. Since the order of the system of differential equations must be matched by the number of boundary conditions, this means that, in the limit $\mathrm{Re} \to \mathrm{Re}_{\rm crit}$ from above, a nonlinear superfluid boundary layer develops. The scaling laws of this boundary layer have not yet been investigated.

It must also be remarked that the boundary conditions described in Sect. 3.2 and used to find nonlinear solutions of the HVBK equations may not be the correct ones (although the computed values of the torque agree with the measurements). A variety of possible boundary conditions have been discussed in the literature [39], encompassing vortex lines sliding perfectly at the walls, being perfectly pinned or partially sliding. The choice made in previous work [25] was motivated by physical simplicity and numerical stability. The fact that it works in the special case of cylindrical geometry (for which in the basic state the vortex lines are parallel to the boundary) may be accidental, as difficulties were found when attempting to solve the HVBK equations in spherical geometry [40].

Rotations of the outer cylinder: The results discussed in this paper refer to rotations of the inner cylinder only and it should be remarked that, when rotating the outer cylinder, a striking observation was made many years ago which still lacks an explanation. Heikkila and Hollis Hallet [41] measured the viscosity of helium II by rotating the outer cylinder at angular velocity Ω_2 and measuring the torque exerted by the fluid on the inner cylinder, which is held stationary. For small values of Ω_2 they reported values of the viscosity (deduced from the measured torque) for $1.13\mathrm{K} < T < T_\lambda$ which are in good agreement with modern values. At moderate values of Ω_2 they found that the expected linear relation between torque and angular velocity breaks, indicating an instability of Couette flow. This result is counter-intuitive because one would expect that the higher the value of Ω_2 the more stable Couette flow is, due to the stratification of angular momentum which is created. Barenghi and Jones [42] proved that, for a pure superfluid ($T = 0$), rotations of the outer cylinder are always unstable due to the vortex tension force. It would be interesting to investigate whether vortex tension is responsible for the findings of Heikkila and Hollis Hallet at finite temperature or whether the observed instability arises from nonlinear effects such as those discussed recently by Richards and Zhang [43] in the astrophysical context.

Instability of Kelvin waves: We mentioned in the introduction that there is current activity to understand the turbulent flow of helium II. Recent work has highlighted the importance to turbulence [44, 45] of an instability which was first observed in the context of heat transfer by Donnelly [46] and then explained by Glaberson and others [47, 48]. The instability takes place when the component of the normal fluid velocity in the direction of the superfluid vortex lines exceeds a critical value. In this case the amplitude of Kelvin waves (helical displacements of the vortex cores), which are initially infinitesimal (being caused by thermal and mechanical

noise), grow exponentially with time; when the amplitude becomes of the order of inter-vortex spacing then neighbouring vortices reconnect and in most cases turbulence is created [8, 49]. With the addition of an axial flow [50] (thus parallel to the superfluid vorticity of the Couette state) the Couette configuration would be ideal to study the Kelvin wave instability in a controlled way, something which evidently cannot be done in the context of a turbulent flow.

References

1. London, F.: *Superfluids*. John Wiley (1954)
2. Khalatnikov, I.M.: *An Introduction to the Theory Superfluidity*. Benjamin (1965)
3. Donnelly, R.J.: *Quantized Vortex Lines in Helium II*. Cambridge University Press (1991)
4. Donnelly, R.J., Barenghi, C.F.: The observed properties of liquid helium at the saturated vapour pressure. J. Physical and Chemical Reference Data **27**, 1217–1274 (1998)
5. Smith, M.R., Donnelly, R.J., Vinen, W.F.: Decay of vorticity in homogeneous turbulence. Physical Review Letters **71**, 2583–2586 (1993)
6. Barenghi, C.F., Swanson, C.J., Donnelly, R.J.: Emerging issues in helium turbulence. Journal of Low Temperature Physics **100**, 385–413 (1995)
7. Maurer, J., Tabeling, P.: Local investigation of superfluid turbulence. Europhys. Lett. **43**, 29 (1998)
8. Finne, A.P., Araki, T., Blaauwgeers, R., Eltsov, V.B., Kopnin, N.B., Krusius, M., Skrbek, L., Tsubota, M., Volovik, G.E.: Transition to superfluid turbulence governed by an intrinsic parameter. Nature **424**, 1022–1025 (2003)
9. Barenghi, C.F., Hulton, S., Samuels, D.C.: Polarisation of superfluid turbulence. Physical Review Letters **89**, 275301 (2002)
10. Landau, L.D., Lifshitz, E.M.: *Fluid Mechanics*. Pergamon (1987)
11. Barenghi, C.F., Donnelly, R.J., Vinen, W.F. (eds.): *Quantized Vortex Dynamics And Superfluid Turbulence*, Springer's Lecture Notes in Physics **571** (2001)
12. Hall, H.E., Vinen, W.F.: The rotation of liquid He II. II the theory of mutual friction in uniformly rotating He II. Proceedings of the Royal Society of London A **238**, 215–234 (1956)
13. Hall, H.E.: The rotation of liquid helium II. Advances in Physics **9**, 89–146 (1960)
14. Bekharevich, I.L., Khalatnikov, I.M.: Phenomenological derivation of the equations of vortex motion in He II. Soviet Phys. JETP **13**, 643–646 (1961)
15. Hills, R.N., Roberts, P.H.: Superfluid mechanics for a high density of vortex lines. Arch Rat Mech Anal **66**, 43–71 (1977)
16. Barenghi, C.F., Donnelly, R.J., Vinen, W.F.: Friction on quantized vortices in He II. A review. Journal of Low Temperature Physics **52**, 189–247 (1983)
17. Taylor, G.I.: Stability of a viscous liquid contained between two rotating cylinders. Phil. Trans. Roy. Soc. Lond. A **223**, 289–343 (1923)
18. Poiseuille, J.L.: Comptes rendus **11**, 961 (1840)
19. Kapitza, P.L.: Journal of Physics, USSR **4**, 181 (1941)
20. Donnelly, R.J., Lamar, M.M.: Flow and stability of helium II between rotating cylinders. Journal of Fluid Mechanics **186**, 163–198 (1988)
21. Swanson, C.J., Donnelly, R.J.: Instability of Taylor–Couette flow of helium II. Physical Review Letters **67**, 1578–1581 (1991)
22. Chandrasekhar, S., Donnelly, R.J.: The hydrodynamic stability of He II between rotating cylinders. I. Proceedings of the Royal Society of London A **241**, 9–28 (1957)
23. Barenghi, C.F., Jones, C.A.: The stability of the Couette flow of helium II. Journal of Fluid Mechanics **197**, 551–569 (1988)
24. Barenghi, C.F.: Vortices and the Couette flow of helium II. Physical Review B **45**, 2290–2293 (1992)
25. Henderson, K.L., Barenghi, C.F., Jones, C.A.: Nonlinear Taylor–Couette flow of helium II. Journal of Fluid Mechanics **283**, 329–340 (1995)
26. Henderson, K.L., Barenghi, C.F.: Numerical methods for helium's two fluid model. Journal of Low Temperature Physics **98**, 351–381 (1995)
27. Henderson, K.L., Barenghi, C.F.: Calculation of the torque in nonlinear Taylor vortex flow of helium II. Physics Letters A **191**, 438–442 (1994)
28. Donnelly, R.J.: Experiments on the hydrodynamic stability of helium II between rotating cylinders. Physical Review Letters **3**, 507–508 (1959)
29. Henderson, K.L., Barenghi, C.F.: The anomalous motion of superfluid helium in a rotating cavity. Journal of Fluid Mechanics **406**, 199–219 (2000)
30. Cliffe, K.A., Mullin, T.: Numerical and experimental study of anomalous modes in the Taylor experiment. Journal of Fluid Mechanics **153**, 243–258 (1985)
31. Schaeffer, D.G.: Qualitative analysis of a model for boundary effects in the Taylor problem. Math. Proc. Camb. Phil. Soc. **87**, 307–337 (1980)
32. Pfister, G., Schmidt, H., Cliffe, K.A., Mullin, T.: Bifurcation phenomena in Taylor–Couette flow in a very short annulus. Journal of Fluid Mechanics **191**, 1–18 (1988)
33. Cliffe, K.A., Kobine, J.J., Mullin, T.: The role of anomalous modes in Taylor–Couette flow. Proceedings of the Royal Society A **439**, 341–357 (1992)

34. Henderson, K.L., Barenghi, C.F.: Transition from Ekman flow to Taylor vortex flow in superfluid helium. Journal of Fluid Mechanics **508**, 319–331 (2004)
35. Bielert, F., Stamm, G.: Visualisation of Taylor–Couette flow in superfluid helium. Cryogenics **33**, 938–940 (1993)
36. Donnelly, R.J., Karpetis, A.N., Niemela, J.J., Sreenivasan, K.R., Vinen, W.F., White, C.M.: The use of particle image velocimetry in the study of turbulence in liquid helium. Journal of Low Temperature Physics **126**, 327–332 (2002)
37. Van Sciver, S.W.: Private Communication (2003)
38. Zhang, T., Celik, D., Van Sciver, S.W.: Tracer particles for application to PIV studeies of liquid helium. Journal of Low Temperature Physics **134**, 985–1000 (2004)
39. Adronikashvili, E.L., Mamaladze, Y.G.: Rotation of helium II. In *Progress in Low Temperature Physics*, volume 5, pages 79–161. C.J. Gorter, North Holland, 1967
40. Hollerbach, R.: Private Communication (2002)
41. Heikkila, W.J., HollisHallett, C.: The viscosity of liquid helium II. Canadian J. Phys. **33**, 420–435 (1955)
42. Barenghi, C.F., Jones, C.A.: The stability of superfluid helium between rotating concentric cylinders. Physics Letters A **122**, 425–430 (1987)
43. Richards, D., Zhang, J.P.: Turbulence in differentially rotating flows: what can be learned from the Taylor–Couette experiment. Astronomy and Astrophysics **347**, 734–738 (1999)
44. Barenghi, C.F., Samuels, D.C., Bauer, G.H., Donnelly, R.J.: Superfluid vortex lines in a model of turbulent flow. Physics of Fluids **9**, 2631–2643 (1997)
45. Samuels, D.C., Kivotides, D.: A damping length scale for superfluid turbulence. Physical Review Letters, **83**, 5306–5309 (1999)
46. Cheng, D.K., Cromar, M.W., Donnelly, R.J.: Influence of an axial heat current on negative ions trapping in rotating helium. Physical Review Letters **31**, 433–436 (1973)
47. Ostermeier, R.M., Glaberson, G.I.: Instability of vortex lines in the presence of axial normal fluid. Journal of Low Temperature Physics **21**, 191–196 (1975)
48. Infeld, E., Lenkowska-Czerwinska, T.: Growth of the normal-flow instability of a vortex array in 2-component He II. Physical Review B **57**, 13390–13392, (1998)
49. Tsubota, M., Araki, T., Barenghi, C.F.: Rotating superfluid turbulence. Physical Review Letters **90**, 205301 (2003)
50. Chandrasekhar, S.: *Hydrodynamic and hydro-magnetic stability*. Dover publications (1961)